

Ca II ABSORPTION LINES IN THE SPECTRUM OF THE QUASAR PKS 2020-370 DUE TO GALACTIC MATERIAL IN THE GROUP KLEMOLA 31

A. BOKSENBERG

Department of Physics and Astronomy, University College London

I. J. DANZIGER AND R. A. E. FOSBURY¹

European Southern Observatory, Munich

AND

W. M. GOSS

Kapteyn Astronomical Institute, University of Groningen

Received 1980 July 21; accepted 1980 September 5

ABSTRACT

In the spectrum of the quasar PKS 2020-370 ($z_{em} = 1.050$), we find Ca II absorption lines both at near zero redshift and at $z_{abs} = 0.02865 \pm 0.00007$. The latter is closely similar to the redshifts of two galaxies in the group Klemola 31, which are nearby on the plane of the sky. This observation adds to the evidence that the narrow-lined heavy-element absorption systems in quasar spectra in general arise in the extended halos of intervening galaxies.

Subject headings: galaxies: redshifts — galaxies: structure — quasars

I. INTRODUCTION

Narrow absorption lines resembling the interstellar lines of our Galaxy are frequently observed in the spectra of quasars and BL Lacertae objects, and the question of their origin has been a matter of much debate in the literature. In principle, the absorbing regions may be intrinsic to these objects, having been somehow ejected at velocities up to the very high values observed ($>0.6c$ in a number of cases), or they may be cosmologically distributed, in direct association with galaxies or as intergalactic clouds. The former has several difficulties, principally the implication of implausibly large mass and momentum flow relative to the quasar (Goldreich and Sargent 1976; Wolfe *et al.* 1976, 1978; Williams and Weymann 1976). On the other hand, from the observed frequency of absorption systems containing heavy elements, if related to galaxies, the effective size of a galaxy seen in absorption must be several times its arbitrary Holmberg dimensions (Bahcall 1975; Burbidge *et al.* 1977; Sargent *et al.* 1979). However, as pointed out by Bahcall and Spitzer (1969), the gas density required to produce absorption lines is so low that it would not be surprising if the maximum dimensions of a galaxy for detectable line absorption were much greater than the dimensions detected in other ways, and they suggested that the observed lines (of heavy-element systems) could be produced in extended, low-density halos of normal galaxies.

The first direct evidence of this came from the detection by Boksenberg and Sargent (1978) of Ca II absorption lines in the spectrum of the quasar 3C 232 ($z_{em} = 0.5303$) close in redshift² to that of the galaxy

¹ Now at Royal Greenwich Observatory, Herstmonceux Castle.

² All redshifts and velocities given here are heliocentric vacuum values.

NGC 3067 ($z = 0.0050$) which lies 1.9 away on the plane of the sky, following the discovery by Haschick and Burke (1975) of H 21 cm absorption in this system. Deep photography showed no trace of spiral arms or other optical features at the location of the absorbing material. Here we present a second, similar case (Danziger and de Jonge 1978): we have detected Ca II absorption lines in the quasar PKS 2020-370 ($z_{em} = 1.050$: our value) at the same redshift as a spiral and an elliptical galaxy in the small group Klemola 31 (Klemola 1969), which lie, respectively, 20" and 45" away on the plane of the sky. A third such detection has now been reported by Blades, Hunstead, and Murdoch (1980) for the quasar 0446-208 and a probable S0 galaxy.

II. OBSERVATIONS

PKS 2020-370 has $m_B = 17.8$ (Peterson and Bolton 1972), which is nominally about 2 mag fainter than 3C 232. We obtained spectra of PKS 2020-370 and the galaxies marked A (a spiral) and B (an elliptical) in Figure 1 (Plate L11) during 1978 August-September with the University College London Image Photon Counting System (Boksenberg 1978) on the Boller & Chivens spectrograph of the European Southern Observatory 3.6 m telescope. Typically, we used an image format of 1500 spectral elements by 70 spatial increments 2' along the slit. Details of the observations are given in Table 1. In all cases the spatial position in the format was periodically interchanged to allow for differences in system response when subtracting the sky component from the object spectra. We concentrated on obtaining high-dispersion (30 \AA mm^{-1}) spectra of the quasar in the blue region where the redshifted Ca II galaxy lines were expected, but also observed the corresponding Na I D-line region (at 60 \AA mm^{-1}). Most of

PLATE L11

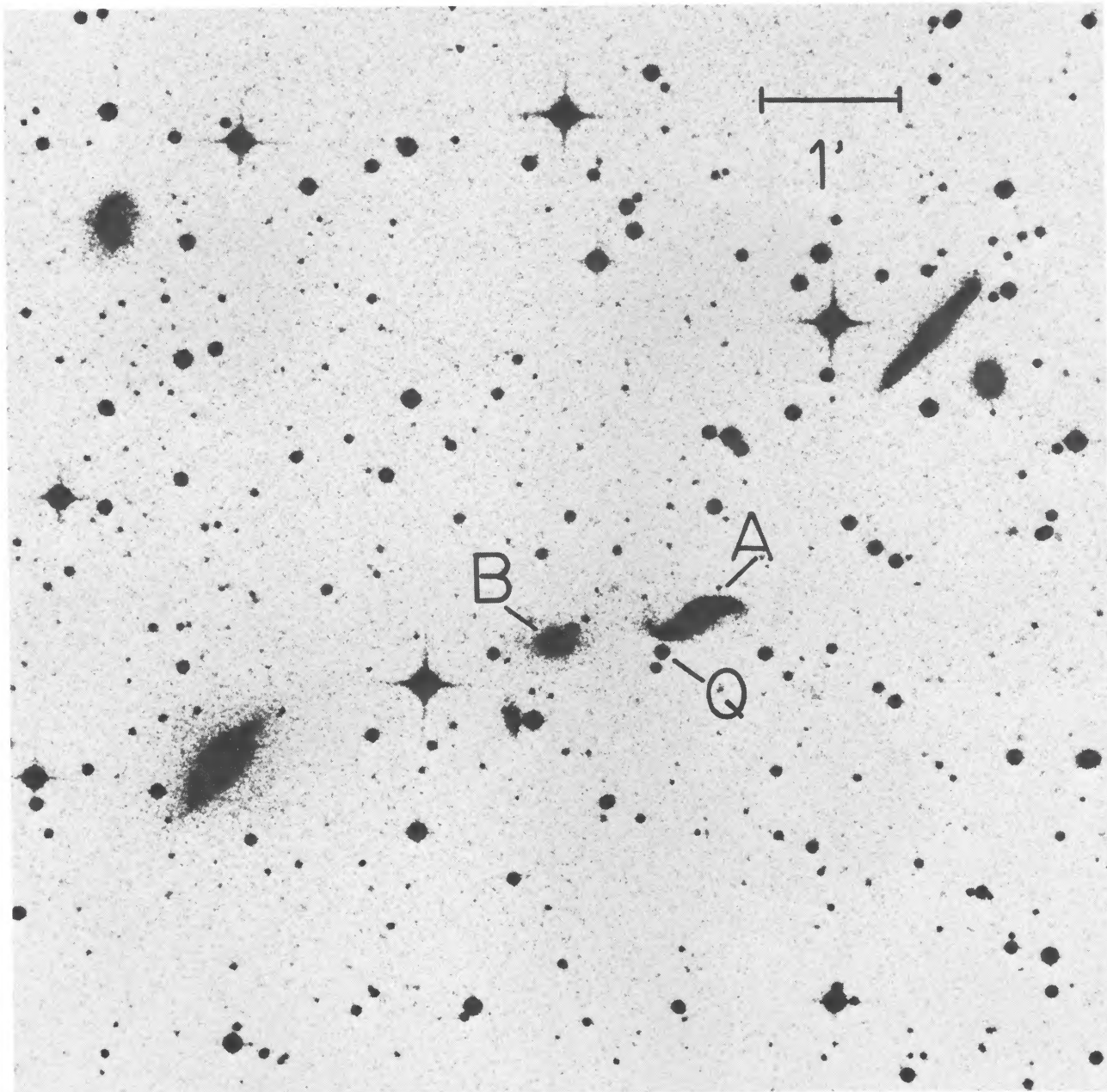


FIG. 1.—Reproduction from a UK Science Research Council IIIa-J plate of the ESO/SRC Southern Sky Survey showing the field of PKS 2020–370 and Klemola 31. North is at the top and east is at the left. The quasar (Q) and the two galaxies discussed in the text are indicated.

BOKSENBURG *et al.* (see page L145)

our data on the Ca II region were obtained on September 1, and some useful but much lower-quality data, in poor observing conditions, on August 26. The total integration on both nights yielded a sky-subtracted continuum count for the quasar $\sim 680 \text{ \AA}^{-1}$. For the observation of September 1, we set the spectrograph slit at position angle 85° to give high-dispersion measurements of galaxy B simultaneously with the quasar and sky. We observed galaxy A at low dispersion (114 \AA mm^{-1}) only.

III. RESULTS

Sections of the high-resolution data for the quasar and galaxy B are shown in Figure 1. The quasar spectrum is the sum of the data from August 26 and September 1; galaxy B is from September 1 only. The spectra are not photometrically corrected; instead, the quasar spectrum is flattened by division with a smooth curve delineating the observed continuum and emission features, while the galaxy spectrum is divided by the quasar continuum only. The low-dispersion spectrum of galaxy A is given in Figure 2, also divided by the quasar continuum. This shows strong Balmer and [O II] emission lines and weaker lines of [O III] and [N II], and in color is relatively blue. In our wavelength range the quasar shows two broad emission lines, C III] and Mg II, which we find, respectively, at $\lambda 3911.2$ and $\lambda 5741.7$; from these we obtain the redshift $z_{\text{em}} = 1.050 \pm 0.002$. For galaxy B we obtain the redshift $z = 0.0285 \pm 0.0001$ from the stellar absorption lines. The redshift of galaxy A, as measured from the H α

and H β emission lines, is closely similar: $z = 0.0288 \pm 0.0002$.

Three definite absorption lines appearing in the spectrum of the quasar over the observed range are listed in Table 2 and are contained in the section reproduced in Figure 1. We identify the line at $\lambda 3933.7$ as Galactic Ca II K at heliocentric velocity (-15 ± 25) km s^{-1} , but the corresponding H line is not obvious. However, the fluctuations over a line width in the continuum near the expected position of the H line corresponding to the velocity of the K line are within the statistical range of equivalent width to be consistent with a Ca II doublet ratio near 2:1. The two other definite lines clearly coincide with the Ca II K and H stellar lines in galaxy B (Fig. 1), and we identify these with Ca II K and H absorption most likely due to outer material associated with galaxy B or A. Although the H line seems to have more structure than the K line, we find (i) the excess is contributed only by the data from one of the two alternate spectral locations exposed on September 1 and does not appear at all in the data of August 26, and (ii) the blue component of the line corresponds well in velocity to the observed K line, but the red component has no appropriate K counterpart. Thus, we have ignored the apparent red component in determining the redshift and equivalent width of the H line as given in Table 2. The mean redshift for both lines is $z_{\text{abs}} = 0.02865 \pm 0.00007$, falling centrally between the redshifts of galaxies A and B. Our nominal values of equivalent width for these lines give the doublet ratio 1.59, but there is a substantial uncertainty which permits all values between 2 and

TABLE 1
JOURNAL OF OBSERVATIONS

Date (UT 1978)	Object	Wavelength Region (\AA)	Slit Width ($''$)	Instru- mental FWHM (\AA)	Integration Time (minutes)
Aug. 26	PKS 2020-370	3850-4750	1.5	1.2	122
Aug. 29	PKS 2020-370	3600-7200	2.0	6.1	9.5
Aug. 29	galaxy A	3600-7200	2.0	6.1	5.5
Sept. 1	PKS 2020-370	3650-4550	2.0	1.5	240
	galaxy B				
Sept. 3	PKS 2020-370	5200-7000	2.0	3.0	140

TABLE 2
ABSORPTION LINES IN THE SPECTRUM OF PKS 2020-370

λ (observed) ^a (\AA)	W_λ (observed) ^b (m \AA)	Identification ^c
3933.7 ± 0.3	320 ± 80	Ca II K Galactic, $v = (-15 \pm 25) \text{ km s}^{-1}$
4046.7 ± 0.3	350 ± 80	Ca II K, $z_{\text{abs}} = 0.0287 \pm 0.0001$
4082.1 ± 0.3	220 ± 80	Ca II H, $z_{\text{abs}} = 0.0286 \pm 0.0001$

^a All wavelengths are air values.

^b The quoted errors in W_λ are rms values due to noise.

^c All derived redshifts and velocities are heliocentrically corrected and calculated from vacuum values of wavelength.

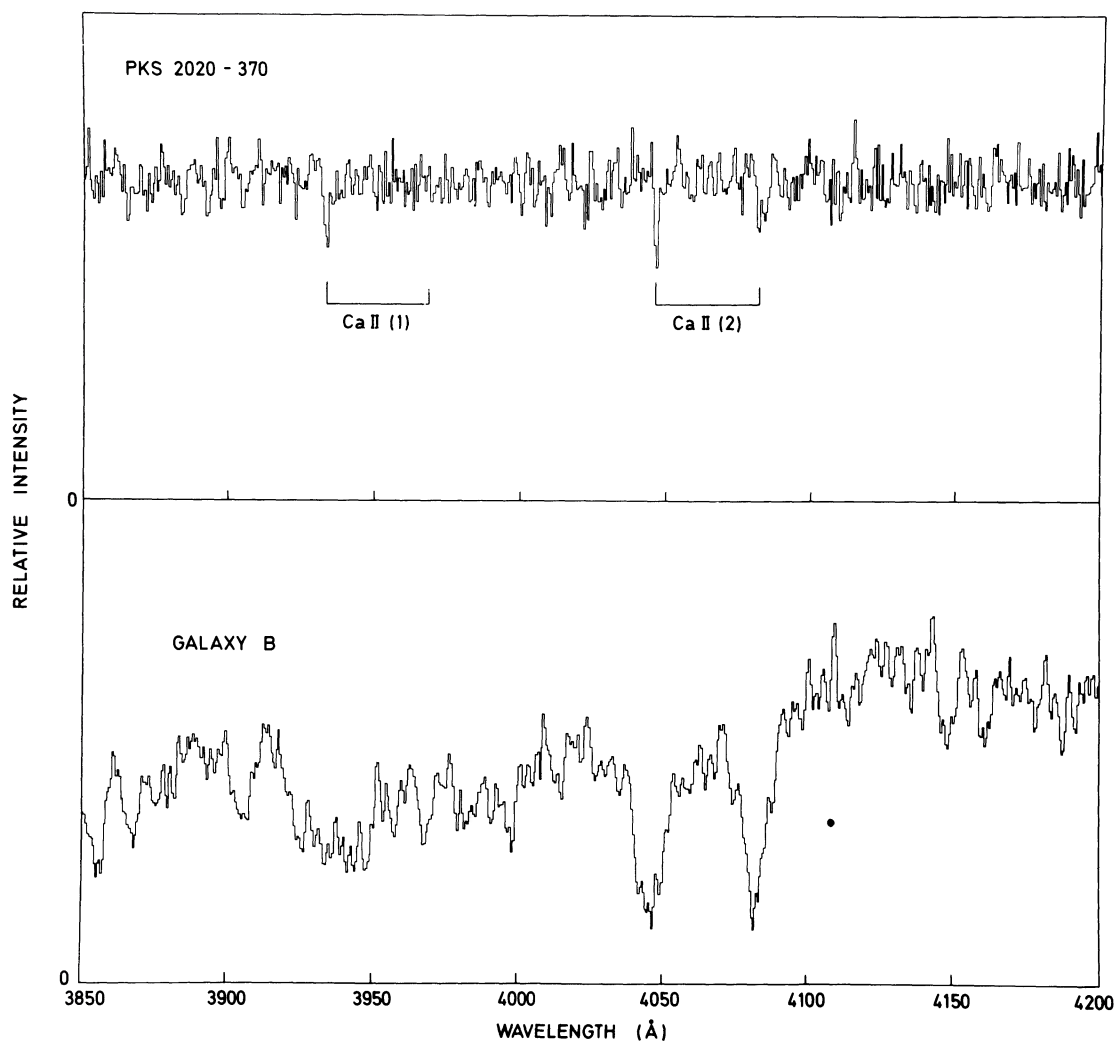


FIG. 2.—Portions of the high-resolution spectra of PKS 2020—370 and a section through the nucleus of galaxy B. The quasar spectrum has been flattened by division with a smooth curve following the observed continuum and emission-line features; the galaxy spectrum is divided by the quasar continuum only. The Galactic (1) and redshifted (2) Ca II absorption lines appearing in the quasar spectrum are indicated.

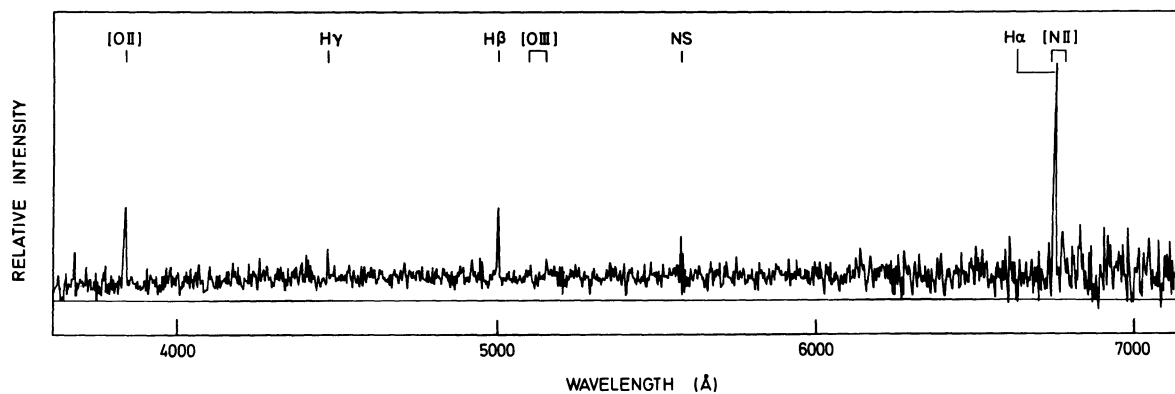


FIG. 3.—Low-resolution spectrum of a section through the nuclear region of galaxy A, divided by the smoothed quasar continuum. Emission lines are identified.

1. Using the tables published by Strömberg (1948), we find for the Ca^+ column density the nominal value $5.5 \times 10^{12} \text{ cm}^{-2}$; the corresponding value for the Doppler parameter b is 15 km s^{-1} . The K line possibly is marginally resolved in our data, and assuming a simple Gaussian velocity profile we estimate $b \lesssim 45 \text{ km s}^{-1}$. The corresponding lower-limit (1σ) value of column density consistent with our data is $2.8 \times 10^{12} \text{ cm}^{-2}$. Although the lines almost certainly have several unresolved components, this result is relatively insensitive to the details of the velocity profile. For the column density of Galactic Ca^+ , we obtain $(3.0 \pm 0.8) \times 10^{12} \text{ cm}^{-2}$, from our observed nominal equivalent width for the K line and assuming the doublet ratio is 2.

Like 3C 232, there are no detectable features at the expected wavelengths of the Na I D lines either near zero velocity or related to galaxies A or B. The 1σ upper limits on equivalent width for D2 are $500 \text{ m}\text{\AA}$ for the former, which has extra noise due to the subtracted Na I night-sky emission, and $250 \text{ m}\text{\AA}$ for the latter. We obtain corresponding upper limits for the Na^0 columns of $2.2 \times 10^{12} \text{ cm}^{-2}$ and $1.1 \times 10^{12} \text{ cm}^{-2}$, respectively, again assuming the doublet ratio is 2.

IV. DISCUSSION

The line of sight to PKS 2020–370 lies $20''$ and $45''$ away from the respective centers of galaxies A and B. The corresponding projected distances are 17 kpc and 37 kpc, if $H_0 = 50 \text{ km s}^{-1} \text{ Mpc}^{-1}$. The nominal recession velocities of the two galaxies both are within about 50 km s^{-1} of that of the high-velocity absorbing material detected in the quasar spectrum, so we cannot relate it preferentially to one or the other.

If the high-velocity absorbing material is associated

with the spiral galaxy (A), the line of sight to the quasar intercepts the outer projections both of the disk and the halo. As in the case of 3C 232 and NGC 3067 (Boksenberg and Sargent 1978), our nondetection of Na I argues for an association with the halo, because in the Galaxy the ratio $N(\text{Ca}^+)/N(\text{Na}^0)$ generally is much larger in the halo than the disk. However, this indication is not conclusive, because (i) similarly large ratios are observed for high-velocity gas in the Galactic plane, and (ii) we have no reason to believe that the generally low values as observed for the inner Galactic disk persist as far as the distant projections of the plane implied for galaxy A and NGC 3067.

It is possible that the observed absorption occurs in the outer halo of the elliptical galaxy (B). The Ca II absorption detected by Blades, Hunstead, and Murdoch (1980) arises in the distant extension of a probable S0 galaxy, which class in general is considered to have a low gas content. Giant shells now have been revealed around several normal elliptical galaxies (Malin and Carter 1980). It would be interesting to attempt the detection of Ca II absorption, in a quasar spectrum, for which an association with a foreground elliptical galaxy is unambiguous.

We thank the technical support group on La Silla for their help in installing the UCL traveling IPCS on the 3.6 m telescope. As usual, particular thanks are due to John Fordham and Keith Shortridge for continuing improvements to the IPCS and to their invaluable and unstinting work in setting it up, maintaining, and operating it over the observing run. The IPCS was developed with the aid of grants from the UK Science Research Council.

REFERENCES

- Bahcall, J. N. 1975, *Ap. J. (Letters)*, **200**, L1.
 Bahcall, J. N., and Spitzer, L. 1969, *Ap. J. (Letters)*, **156**, L63.
 Blades, J. C., Hunstead, R. W., and Murdoch, H. S. 1980, *M.N.R.A.S.*, in press.
 Boksenberg, A. 1978, ESO Conf., *Optical Telescopes of the Future*, December 12–15, Geneva, p. 497.
 Boksenberg, A., and Sargent, W. L. W. 1978, *Ap. J.*, **220**, 42.
 Burbidge, G. R., O'Dell, S. L., Roberts, D. H., and Smith, H. E. 1977, *Ap. J.*, **218**, 33.
 Danziger, I. J., and de Jonge, M. J. 1978, *ESO Messenger*, No. 15, p. 19.
 Goldreich, P., and Sargent, W. L. W. 1976, *Comments Astr. Ap.*, **6**, 133.
 Haschick, A. D., and Burke, B. F. 1975, *Ap. J. (Letters)*, **200**, L157.
 Klemola, A. R. 1969, *A.J.*, **74**, 804.
 Malin, D. F., and Carter, D. 1980, *Nature*, **285**, 643.
 Peterson, B. A., and Bolton, J. G. 1972, *Ap. Letters*, **10**, 105.
 Sargent, W. L. W., Young, P. J., Boksenberg, A., Carswell, R. F., and Whelan, J. A. J. 1979, *Ap. J.*, **230**, 49.
 Strömberg, B. 1948, *Ap. J.*, **108**, 242.
 Williams, R. E., and Weymann, R. J. 1976, *Ap. J. (Letters)*, **207**, L143.
 Wolfe, A. M., Broderick, J. J., Condon, J. J., and Johnston, K. J. 1976, *Ap. J. (Letters)*, **208**, L47.
 ———. 1978, *Ap. J.*, **222**, 752.

A. BOKSENBERG: Department of Physics and Astronomy, University College London, Gower Street, London WC1E 6BT, England

I. J. DANZIGER: European Southern Observatory, Karl Schwarzschild Strasse 2, 8046 Garching bei München, Germany

R. A. E. FOSBURY: Royal Greenwich Observatory, Herstmonceux Castle, Hailsham, East Sussex BN27 1RP, England

W. M. GOSS: Kapteyn Astronomical Institute, University of Groningen, Postbus 800, NL-9700 AV Groningen, The Netherlands